



# Extending the Sensitivity of Air Čerenkov Telescopes

I. de la Calle Perez and Steve D. Biller

Department of Physics, University of Oxford, Keble Road, Oxford OX1 3RH, UK

**Abstract.** Over the last decade, the Imaging Air Čerenkov technique has proven itself to be an extremely powerful means to study very energetic gamma-radiation from a number of astrophysical sources in a regime which is not practically accessible to satellite-based instruments. With the current generation of Čerenkov telescopes well on their way, effort has been shifted now towards a further improvement of the capabilities of these instruments. Here we present a practical method to substantially improve the sensitivity of Atmospheric Čerenkov Telescopes above 1 TeV using wide-angle cameras with a relatively coarse density of photomultiplier tubes. The results are presented in terms of the performance of a single and an array of two wide-angle telescopes.

## 1. Introduction

The Imaging Atmospheric Čerenkov Telescope (ACT) has proven to be a highly successful technique in the detection of high energy, gamma-rays from astrophysical sources above  $\sim 250$  GeV. The catalogue of TeV sources is fast increasing and includes mainly supernova remnants (SNR) (see e.g. Weekes et al. 1989; Aharonian et al. 2001; Aharonian et al. 2005c) and active galaxies (AGN) (see e.g. Horan et al. 2004 and references therein), although recently, new classes of objects such as OB star associations (Aharonian et al. 2002) and binary systems (Aharonian et al. 2005a), have been confirmed to be sources of high energy gamma-rays. Also, a recent survey of the galactic plane has yielded a significant signal from the region of the galactic centre (Aharonian et al. 2004a) and the discovery of a series of objects lying along the galactic plane (Aharonian et al. 2005b). The nature of the physics addressed via high energy gamma-ray measurements includes clues to the understanding of the origin of cosmic rays, the nature of AGN jets and the density of the extragalactic infrared background. In addition, several fundamental topics of particle physics can be probed, including searches for TeV-scale WIMP annihilations (see Buckley et al. 1998 and references therein), limits on radiative neutrino decay (Biller et al. 1998) and a fundamental test of Lorentz invariance based on studies of the propagation of very high energy radiation over extragalactic distances (Biller et al. 1999b). The sensitivities of such searches are among the very best achieved by any technique.

Almost all current ground-based gamma-ray efforts have concentrated primarily on improving the sensitivities to lower energies so as to overlap more with satellite-based observations and potentially map out a larger range of sources. However, it is of interest to note that many of the physics topics mentioned above actually stand to benefit most from improved measurements at higher energies. It is in this regime where AGN spectra and short timescale flux variability most critically test acceleration mechanisms as well as uniquely probe the extragalactic infrared back-

ground radiation. These higher energy emissions permit the direct study of some of the most extreme and poorly understood environments in the universe. There are now several sources known to produce gamma-ray emission in the regime above 10 TeV, with evidence of some producing gamma-ray emission up to 40 TeV (see e.g. Aharonian et al. 2005c), and potentially as high as 100 TeV (Aharonian et al. 2004b). Establishing the actual range of this emission would, in itself, be of substantial interest. Furthermore, it is generally acknowledged that much greater sky coverage is desired to study extended sources (Aharonian et al. 2005c), to better explore the gamma-ray sky and to more continuously monitor multiple sources to study transient behaviour.

The approach taken in this work involves the use of cameras with a relatively large field of view ( $\sim 10^\circ$ ), which has the additional advantage of acting as a test-bed for the development of “all-sky” instruments. While initially motivated to improve the sensitivity at higher energies ( $>1$  TeV), the approach is seen to lead to improvements for energies at least as low as 300 GeV.

## 2. The concept of a Wide Angle Camera

The Čerenkov lateral distribution of TeV gamma-ray induced showers presents a well defined plateau of nearly constant photon density up to a distance of  $\sim 120$  m, after which the photon density falls off rapidly, making it more difficult to trigger a Čerenkov telescope. However, substantial levels of light are produced at large core distances for high energy showers (Fig. 1). From this figure it can be extracted that the ability to trigger on 1 TeV showers at core distances beyond  $\sim 100$  m implies the ability to see 10 TeV showers beyond  $\sim 400$  m. However, the image centroid for such showers would be displaced nearly  $4^\circ$  from the source position (Fig. 2). This indicates that in order to take advantage of the potential increase in effective area that this offers, a large field of view is required. However, several issues, such as optical aberrations, image rejection and energy resolution, have to be addressed first. In par-

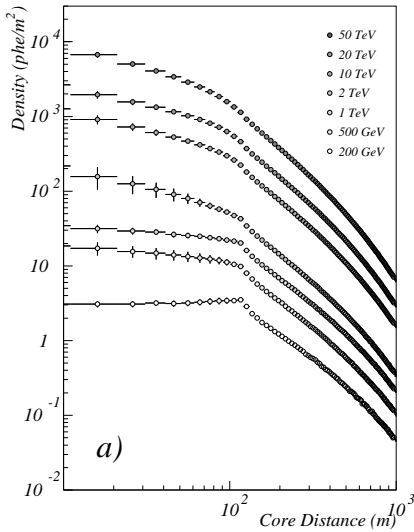


**Fig. 1.** Simulated average Čerenkov lateral distribution for showers initiated by gamma-rays of various energies, convolved with atmospheric extinction, mirror reflectivity and typical photomultiplier tube efficiency. All simulated showers were generated from a zenith angle of  $0^\circ$  with an assumed observation level for detection of 2400 m above sea level.

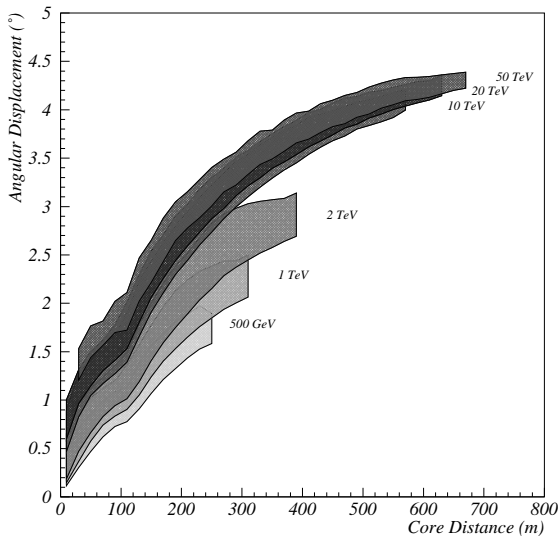


**Fig. 2.** Image angular displacement ( $\mathcal{D}$ ) as a function of core distance for 0.5, 1, 2, 10, 20 and 50 TeV gamma-ray showers. The shaded bands include 68% of the events about the median.

ticular, the improvement of background rejection becomes necessary. The lower image intensities for events at large core distances, means that the hadronic background will be higher for these events due to the strong energy dependence of the cosmic-ray spectrum. Also, the image position in the camera relative to the source location increases at large core radii due to geometric effects and image rejection is unproven in this regime.

### 3. Simulations

The EAS shower and detector simulation package<sup>1</sup> has been used to generate gamma-ray and cosmic-ray induced showers (see Table 1). For the purpose of some plots, a set of gamma-ray showers have also been generated with fix energies up to 100 TeV.

|   | Number of Showers | Energy Range | Core Distance Range | Integral Spec. Ind. |
|---|-------------------|--------------|---------------------|---------------------|
| G | $4.8 \cdot 10^6$  | 0.3-20 TeV   | 0.-800. m           | 1.5                 |
| P | $9.6 \cdot 10^6$  | 0.2-20 TeV   | 0.-800. m           | 1.7                 |

**Table 1.** Summary of Shower Simulations. Showers have been uniformly thrown over the indicated area around the detector. The Gamma (G) showers are thrown from the zenith, Proton (P) showers are simulated uniformly in solid angle up to  $15^\circ$  in zenith angle. Every simulated shower is used 100 times.

A  $f=1.0$  optical reflector of 10 m diameter with a 935 pixel camera ( $0.3^\circ/\text{pixel}$ ) covering a  $10^\circ$  field of view (FOV) has been simulated. The optical reflector simulated in this work shows a point spread function (PSF) of  $\sigma_{PSF} = 0.067^\circ$  at the centre of the camera and  $\sigma_{PSF} = 0.22^\circ$  off-centred by  $4.5^\circ$ . The ability to reconstruct the image angular size it is not affected by the PSF (see de la Calle et al. 2006). Mirror reflectivity and photomultiplier (PMT) QE curves similar to those of the Whipple 10 m telescope have been used. 80% reflectivity light cones have also been included. A simple trigger of any two pixels with a signal  $\geq 20$  d.c. is assumed (where 1 d.c./ph.e here) A 2 level image cleaning and image parametrisation, where at least 5 picture pixels are required in the image, has been applied to characterise simulated images similar to that employed by the Whipple group (see Reynolds et al. 1993). We have made use of a new parameter,  $\mathcal{T}_S$ , defined as the time gradient of the image along the camera, for gamma-hadron rejection and energy reconstruction. For the purposes of this work, the image cuts have been chosen as a function of the image size and angular distance such as to arbitrarily keep 95% of the gamma-ray showers after applying each cut in width, length,  $\mathcal{T}_S$  and alpha. The combination of the individual image cuts yields a 75% gamma-ray acceptance and  $\sim 99.8\%$  background rejection.

One obvious way to gain further background rejection and also improved energy resolution is with the use of multiple telescopes. A tandem configuration in which identical wide-angle ACTs are separated by 125 m (close to the optimum distance suggested by Aharonian et al. 1997 based on trigger rates) has been explored in this work. We will refer to the stand alone wide-angle telescope as WFOV-1 while WFOV-2 will refer to the tandem telescope just described.

<sup>1</sup> EAS has been developed by S. D. Biller and is based on EGS4 and SHOWERSIM.

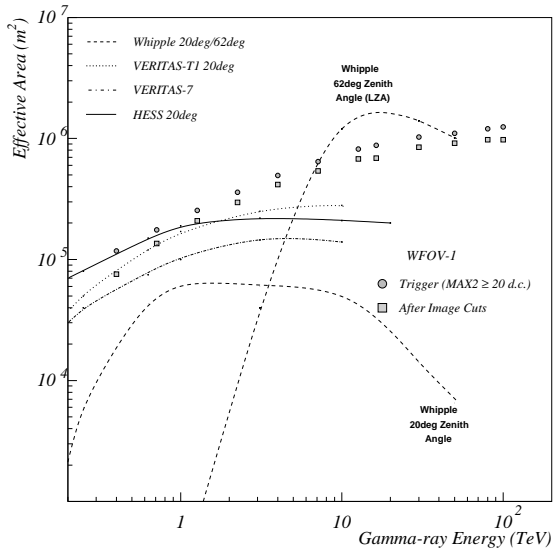


**Fig. 3.** Gamma-ray collection areas at the trigger level and after image cuts for the WFOV-1. The different lines correspond to effective areas after image cuts for Whipple-490 and Whipple-490 at Large Zenith Angle (LZA) (Petry et al. 2001) (dashed line), HESS (Benbow et al. 2005) (continuous line) and VERITAS-T1 (Maier et al. 2005) (dotted line), VERITAS-7 (Weekes et al. 2002) (dotted-dashed line).

## 4. Results

### 4.1. Effective Area and Gamma-ray Rates

Figure 3 shows the derived effective area for gamma-ray showers as a function of the true primary energy for triggered showers both before and after image selection. The effective collection area for gamma-rays after this selection is  $\sim 2 \times 10^5$  m<sup>2</sup> at primary energies of 1 TeV and exceeds  $\sim 5 \times 10^5$  m<sup>2</sup> above 5 TeV. A comparison with the Whipple 10 m gamma-ray telescope, which is similar to the detector simulated here, shows that an increase of a factor  $\sim 3$  at 1 TeV and  $\sim 10$  above 5 TeV is possible.

The convolution of the gamma-ray collection areas with a power-law spectrum of index 2.5 gives the differential rates. Integrating to infinity, rates of 3.35  $\gamma$ /min and 0.33  $\gamma$ /min are obtained above 1 TeV and 10 TeV respectively.

For proton-induced showers the effective collection area is suppressed by roughly a factor of  $10^3$  following image selection. It has to be kept in mind that the resolution of “equivalent” gamma-ray energies and their effect on assumed background and source spectra must be taken into consideration.

### 4.2. Energy Resolution

A  $\chi^2$  minimisation method has been employed to simultaneously reconstruct the core position and gamma-ray energy of each event so as to explore resolution properties of the hypothetical ACT. Three image characteristics were used in this fit:  $D$ ,  $\log_{10}(S)$  and  $\log_{10}(T_S/D)$ , where

$D$  refers to angular distance and  $S$  to the image size in digital counts. To define the  $\chi^2$  model, simulated gamma-ray events were first categorised into 10 m intervals of core distance and logarithmic intervals of primary gamma-ray energy using 10 bins per decade above 300 GeV. Using an independent simulated data set from that used to generate the model, this  $\chi^2$  was then minimised with respect to  $E$  and  $R$  for each event using values from the 2-D matrix described above.

We find energy resolutions of the order of 25% above 1 TeV, independently of true gamma-ray energy or true core location (the energy resolution has been defined as  $(E_{Rec} - E_T)/E_T$ , where  $T$  stands for *True* and  $Rec$  for *Reconstructed*). This is comparable to what single telescopes, like the Whipple telescope, can achieve.

The  $\chi^2$  approach for determining primary energy and core location was modified for the 2-telescope case to simultaneously fit both camera images. We fit for the 2-D core location plus primary gamma-ray energy. Also, a new parameter, the angular deviation between the core direction and the direction of the image centroid, both relative to the centre of the particular camera (which is assumed to track the source), has been introduced. Following a similar fitting procedure as in the case of a single telescope, an energy resolution of  $\sim 20\%$  is achieved.

### 4.3. Sensitivity

The image selection and energy reconstruction procedures previously described were applied to simulated gamma-ray and proton spectra sampled from differential power laws of the form  $E^{-2.5}$  and  $E^{-2.7}$ . The simulated spectra were normalised accordingly to the measured high energy flux from the Crab Nebula near 1 TeV and to cosmic ray primary measurements and convolved with the relevant effective collection areas. This yields differential detection rates in terms of the reconstructed, effective gamma-ray energy ( $E_{Rec}^\gamma$ ). The sensitivity will be defined based on the integrated signal above a given effective energy threshold which yields a detection at a significance level of  $5\sigma$  and a minimum of 10 detected high-energy gamma-rays.

The resulting sensitivity curves as a function of  $E_{Rec}^\gamma$  are shown in Fig. 4 and Fig. 5 for exposure times of 50 hours and 1 hour respectively. For continuous sources based on 50 hours of exposure, the wide-angle camera is found to be approximately a factor of two more sensitive than the Whipple instrument, even at energies as low as 300 GeV. The device becomes comparable to VERITAS and HESS at energies above 10 TeV, despite backgrounds, owing to the greatly increased collection area. For 1 hour exposure times, the wide-angle camera surpasses the sensitivity of the arrays above 2-3 TeV, despite being only a single telescope with a  $\sim 30\%$  smaller mirror area than each element of the arrays. This is due to the fact that, with a much larger collection area, the wide-angle camera tends to be background dominated rather than statistics limited. Thus, any decrease in the relative background

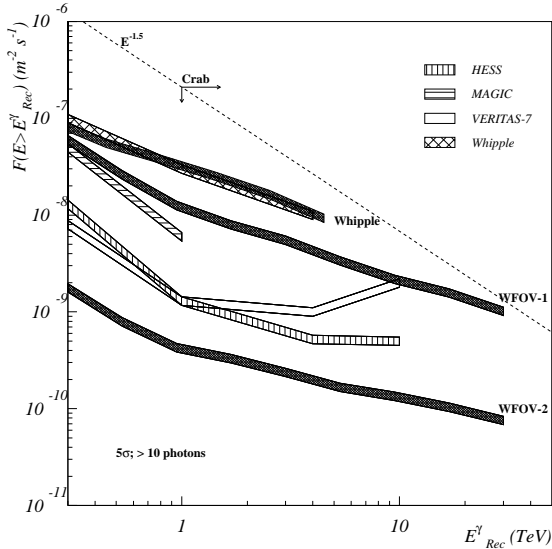


**Fig. 4.** Integral sensitivity curve for the WFOV-1 and WFOV-2 for a 50 h exposure assuming an integral  $E^{-1.5}$  source spectrum. Also shown is the sensitivity curve for a Whipple-like detector derived using the same simulation software used to explore the wide-angle telescope considered in this work. These are compared with the stated sensitivity curves for other experiments from Weekes et al. (2002) and Hofmann et al. (2001).

level (whether through improved background rejection or higher source fluxes over shorter exposure times) results in greater improvement relative to conventional cameras, which become starved for signal above  $\sim 1$  TeV.

Following a similar procedure, for the 50 hour exposure, the sensitivity of the tandem wide-angle design is a factor of  $\sim 4$  times more sensitive over the range above 300 GeV, with extended sensitivity above 10 TeV. For the case of 1 hour exposure, relevant for episodic sources, such as AGN, the sensitivities are comparable at 300 GeV, exceed an order of magnitude improvement in sensitivity above 5 TeV and is significantly more sensitive in the regime above 10 TeV.

## 5. Conclusions

The study presented here suggests that cameras with much larger fields of view than the ones employed by current ACT detectors have the potential of substantially improved their sensitivity in the regime above 300 GeV for the same PMT density that are currently employed. The ability to image showers further “off-axis” leads to a significant gain in effective area with no significant loss in energy resolution compared with current instruments, even for showers with cores landing much further from the telescopes. The ability to suppress background events also appears to be substantial for such a design and yields a very good sensitivity over a remarkably large dynamic range. This background rejection has been enhanced by the introduction of additional imaging parameters based on both intra- and inter- telescope timing characteristics.

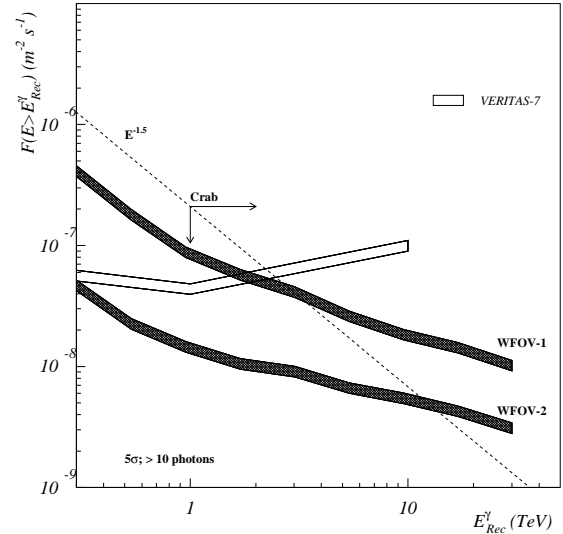


**Fig. 5.** Scaled 1 h integral sensitivity curves for the WFOV-1 and WFOV-2 assuming an integral  $E^{-1.5}$  source spectrum. Also shown is the expected response of VERITAS-7 for a 1 h exposure.

The greater background suppression offered by a telescope array combined with the use of wide angle detector allows the study of sub-hour scale events with unprecedented statistics at TeV energies. Another advantage of using a wide angle camera, is a greater sky coverage, which is roughly an order of magnitude larger than existing instruments. The details of the study presented here can be found in de la Calle et al. (2006).

*Acknowledgements.* This research has been supported by the Particle Physics and Astronomy Research Council (PPARC).

## References

- Aharonian, F. A., et al., 2005a, A&A, 442, 1
- Aharonian, F. A., et al., 2005b, Science, 307, 1839
- Aharonian, F. A., et al., 2005c, A&A, 437, L7
- Aharonian, F. A., et al., 2004a, A&A, 425, 13L
- Aharonian, F. A., et al., 2004b, ApJ, 614, 897
- Aharonian, F. A., et al., 2002, A&A, 393, 37L
- Aharonian, F. A., et al., 2001, A&A, 370, 112
- Aharonian, F. A., et al., 1997, Astroparticle Physics, 6, 343
- Benbow, W. et al., et al., 2005, 2nd High Energy Gamma-ray Symposium, AIP Conference Proceedings, 745, 611
- Biller, S. D., et al., 1999, Physical Review Letters, 83, 2108
- Biller, S. D., et al., 1998, Physical Review Letters, 80, 14
- Bergström, L., Ullio, P. and Buckley, J. H., 1998, Astroparticle Physics, 9, 137
- de la Calle Pérez, I. & Biller, S. D., 2006, Astroparticle Physics, 26, 69
- Hofmann, W., et al., 2001, 27th ICRC, Hamburg, 7, 2785
- Horan, D. & Weekes, T. C., 2004, NewAR, 48, 527
- Maier, G., et al., 2005, 29th ICRC, Pune, , 101
- Petry, D., et al., 2001, 27th ICRC, Hamburg, 7, 2848
- Reynolds, P. T., et al., 1993, ApJ, 404, 206
- Weekes, T. C., et al., 2002, Astroparticle Physics, 17, 221
- Weekes, T. C., et al., 1989, ApJ, 342, 379